



# Chiral 1,1'-Binaphthyl-2,2'-Dithiol-Stabilized Gold Clusters: Size Separation and Optical Activity in the UV-vis

CYRILLE GAUTIER,<sup>1</sup> ROSSANA TARAS,<sup>2</sup> SERAFINO GLADIALI,<sup>2</sup> AND THOMAS BÜRGI<sup>1\*</sup>

<sup>1</sup>Université de Neuchâtel, Institut de Microtechnique, Rue Emile-Argand 11, 2009- Neuchâtel, Switzerland

<sup>2</sup>Dipartimento di Chimica, Università di Sassari, Via Vienna 2, 07100 Sassari, Italy

*Dedicated to Professor Nina Berova on the occasion of her significant anniversary and her receiving the Chirality Medal 2007.*

**ABSTRACT** Gold particles covered with 1,1'-binaphthyl-2,2'-dithiol (BINAS) were prepared. Using size exclusion chromatography, it was possible for the first time to separate the sample into fractions with different sizes and colors. Transmission electron microscopy shows that the particles are very small, in the order of 1 nm or slightly above. The absorption spectra of the separated samples show rich structure. The particles show size-dependent optical activity in metal-based electronic transitions. The shape of both the absorption and circular dichroism spectra of one of the smallest fractions exhibits similarities with the spectra reported for Au<sub>11</sub> covered by 2,2'-bis(diphenylphosphino)-1,1'-biphenyl although the spectra are shifted to shorter wavelengths in the case of the dithiol. The anisotropy factors,  $\Delta\epsilon/\epsilon$  of these particles are as large as  $4 \times 10^{-3}$ , which is larger than the values reported for gold particles stabilized by phosphines and water-soluble thiols. This indicates that BINAS is particularly well-suited to impart chirality on to gold particles. *Chirality* 20:486–493, 2008. © 2007 Wiley-Liss, Inc.

**KEY WORDS:** circular dichroism; optical activity; 1,1'-binaphthyl-2,2'-dithiol; nanoparticles; gold; size separation

## INTRODUCTION

Monolayer protected nanoparticles (MPNs) are fascinating hybrid materials composed of a metallic core surrounded by an organic monolayer.<sup>1</sup> Their physical and chemical properties can easily be tuned for custom requirements by changing their size and by modifying in a judicious way the organic shell. Their potential applications were reported in various fields such as catalysis,<sup>2</sup> sensing,<sup>3,4</sup> therapy,<sup>5</sup> electronics,<sup>6</sup> and optics.<sup>7</sup> Among the huge number of different particles, the subnanometer range of inorganic–organic hybrid nanoparticles has gained great interest both in fundamental and applied research. This class of material exhibits strong size-dependant properties.<sup>8,9</sup> From a fundamental point of view, these particles can be understood as an intermediate state of matter between a single metal atom and a bulk metal. As such they serve as models to understand fundamental physical properties like quantum confinement and structural evolution. Their solubility in various solvents makes them amenable to size separation and spectroscopic techniques which are of great help in elucidating the size dependence of their physical properties. MPNs can also be viewed as the nanometer size analogue of self-assembled monolayers (SAMs) on extended metal surfaces and are a powerful tool for a better understanding of the interaction between metal surfaces and organic molecules.

Recently, the use of chiral passivating agents was considered. To probe the chiral nature of these particles,

chiroptical techniques such as circular dichroism (CD) and vibrational circular dichroism (VCD) are particularly helpful. Based on the comparison between the experimental and calculated VCD spectra, the preferential conformation of *N*-acetyl-cysteine<sup>10</sup> and *N*-isobutyryl-cysteine<sup>11</sup> absorbed on gold particles was proposed. These results were in good agreement with those obtained from measurements on a SAM of the thiol on extended gold surfaces.<sup>12</sup> Furthermore, the use of a chiral capping agent leads to optical activity located in metal-based electronic transition.<sup>11,13–19</sup> This shows that chirality can be bestowed to the metal. However, the question whether the metal core adopts an intrinsically chiral structure<sup>20</sup> or whether the chirality is only imposed on to the electronic structure of the metal core<sup>21</sup> remains still unanswered.

The optical activity located in metal-based transitions is promising for applications in the field of asymmetric reactions catalyzed by small metal nanoparticles. Tamura and Fujihara have reported the asymmetric hydrosilylation of styrene with trichlorosilane catalyzed by chiral palladium

Contract grant sponsors: Swiss National Science Foundations, Swiss National Supercomputer Centre (Manno)

\*Correspondence to: Thomas Bürgi, Université de Neuchâtel, Institut de Microtechnique, Rue Emile-Argand 11, 2009- Neuchâtel, Switzerland.

E-mail: thomas.burgi@unine.ch

Received for publication 13 April 2007; Accepted 11 September 2007

DOI: 10.1002/chir.20488

Published online 25 October 2007 in Wiley InterScience (www.interscience.wiley.com).

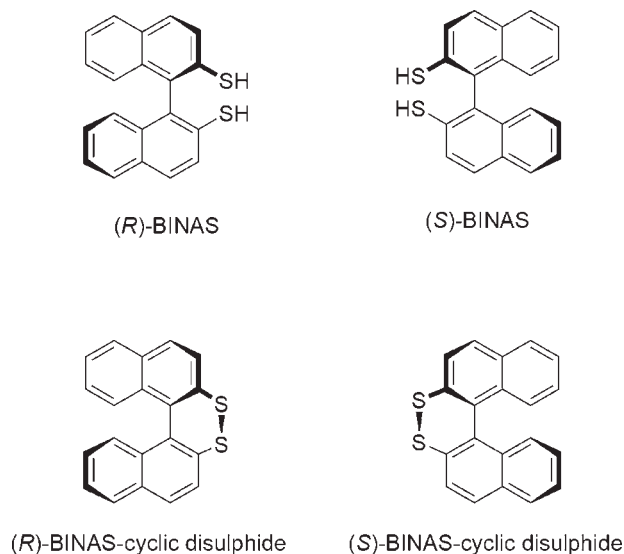


**Chart 1.** Structure of (R)-BINAS, (S)-BINAS, (R)-BINAS-cyclic disulphide, and (S)-BINAS-cyclic disulphide.

nanoparticles stabilized by optically active 2,2'-bis(diphenylphosphino)-1,1'-binaphthyl (BINAP).<sup>16</sup>

Catalysis by gold nanoparticles is evolving very rapidly. Gold is established to be effective as heterogeneous and homogeneous catalyst in hydrogenation, in selective oxidation, in nucleophilic addition to  $\pi$  systems and for many reactions for which a catalyst had not been previously identified.<sup>22</sup> Thus chiral gold nanoparticles are expected to be of great interest in the field of enantioselective catalysis.

Here we report the preparation and chiroptical properties in the UV-vis of gold nanoparticles covered by the two enantiomeric forms of an atropisomeric dithiol: (R)-1,1'-binaphthyl-2,2'-dithiol [(R)-BINAS] and (S)-1,1'-C1 binaphthyl-2,2'-dithiol [(S)-BINAS]<sup>23</sup> (Chart 1). Size exclusion chromatography (SEC) allowed, for the first time, the separation of up to five different fractions with well-defined and distinctly different absorption spectra and colors. The five separated fractions showed strong optical activity in metal based electronic transitions. The origin of this optical activity is discussed.

## MATERIALS AND METHODS

### Materials

The preparation of enantiomerically pure (R)- and (S)-BINAS was reported elsewhere.<sup>23</sup> Deuterated chloroform (99.8%) was received from Cambridge Isotope Laboratories. Gold(III) chloride trihydrate ( $\text{HAuCl}_4 \cdot 3\text{H}_2\text{O}$ , 99.99%), sodium borohydride ( $\text{NaBH}_4$ , 98%) and tetraoctylammonium bromide (TOAB, >98%) were purchased from Aldrich, chloromethylated styrene-divinyl benzene (99:1) resin was obtained from Bio-Rad, Richmond, CA (Bio-Beads SX1, 200–400 mesh). Water was purified with a Milli-Q system ( $\geq 18 \text{ M}\Omega \text{ cm}$ ). Tetrahydrofuran (THF) and dichloromethane were distilled under nitrogen to

remove dissolved oxygen. All other chemicals were analysis grade and were used as received.

### Synthesis of Gold BINAS MPNs

(R)-BINAS and (S)-BINAS MPNs were both prepared under anaerobic conditions following the two-phase method of Brust et al.<sup>24</sup> Briefly, to a vigorously stirred solution of tetrachloroauric acid (132 mg, 0.335 mmol) in 6 ml of deaerated Milli-Q (sonication under vacuum) was added 183 mg of TOAB (0.335 mmol) dissolved in 10 ml of distilled dichloromethane. The mixture was stirred for 30 min. The phase transfer of gold salts from water to dichloromethane results in a discoloration of the aqueous phase and imparts an orange color to the organic phase. The two phases were allowed to settle. Then, the orange organic phase was removed and added to 214 mg (0.67 mmol) of the corresponding enantiomer of BINAS dissolved in 100 ml of distilled dichloromethane. After 30 min, the solution was reduced by addition of a freshly prepared aqueous  $\text{NaBH}_4$  solution (5 ml, 317 mg, 8.38 mmol) under vigorous stirring. The mixture was allowed to react over night under an argon atmosphere. The resulting dark organic solution was extracted and washed three times with water. The solution was dried over  $\text{Na}_2\text{SO}_4$  and filtered using a 0.2- $\mu\text{m}$  PTFE membrane to remove insoluble material. The filtrate was evaporated to near dryness at 40°C and the nanoparticles were precipitated several times with a large excess of hexane and filtered using the same 0.2  $\mu\text{m}$  PTFE membrane. Purification of BINAS gold nanoparticles was repeated until no free BINAS, disulfur, or phase transfer catalyst were detected by  $^1\text{H}$  NMR. We obtained finally 176 mg of gold nanoparticles protected with a monolayer of the corresponding enantiomer of BINAS.

### Separation of Gold BINAS MPNs by SEC

The THF used for elution and for packing the column was freshly distilled under nitrogen and protected from atmospheric contamination. Bio-Beads S-X1 beads were placed in THF (six times the resin weight). The resin was allowed to swell overnight and packed in a glass column (1.2 m length and 2 cm in diameter). The column was washed with several bed volumes of solvent after packing and between separations. For size separation, the sample (90 mg) was dissolved in a minimum amount of distilled THF and loaded on the column. The elution was done with THF at a flow rate of ca. 0.5 ml/min and 5 ml fractions were collected. Each fraction was controlled by UV-vis spectrometry and classified according to its absorption profile.

### Characterization of the Particles by UV-vis, CD, and NMR Spectroscopy

$^1\text{H}$  NMR spectra of the as prepared particles were measured on a Bruker Avance 400 MHz spectrometer at room temperature. Solutions were prepared in  $\text{CDCl}_3$  at a concentration of  $\sim 50 \text{ mg/ml}$ . UV-vis and CD spectra, respectively, of the separated particles were collected on a

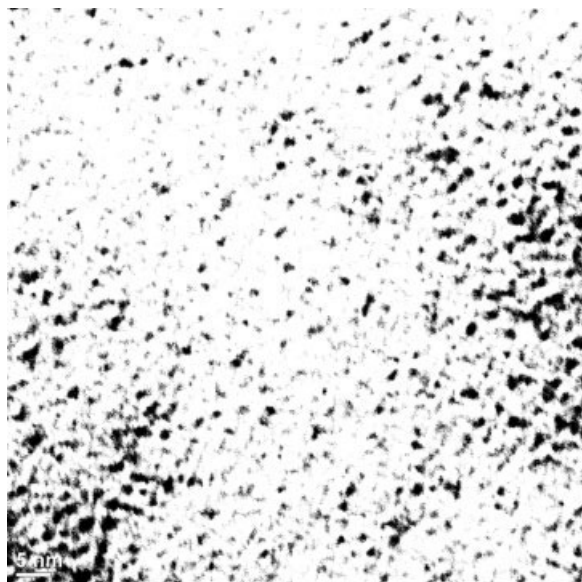


**Fig. 1.** TEM micrograph of gold BINAS MPNs fraction 1.

Cary 300 and a Jasco 710 spectrometer, respectively, using a quartz cell of 1-cm path length and solutions of about 0.3 mg/ml in THF.

### *Transmission Electron Microscopy*

Transmission electron microscopy (TEM) images were recorded with a Philips C200 electron microscope operated at 200 kV. The nanoparticles were dissolved in dichloromethane ( $\sim 0.5$  mg/ml). TEM samples were prepared by casting a drop of the solution onto a carbon-coated copper grid.

## **RESULTS AND DISCUSSION**

### *Size Separation of Gold BINAS MPNs*

The as-prepared product consists of gold BINAS MPNs with an average size smaller than 2 nm as shown by the TEM (see Fig. 1) and confirmed by the absence of a plasmon resonance band at around 520 nm in UV-vis (see Fig. 2). This type of small gold MPNs has a typical molecular weight range between 4 and 20 kDa,<sup>17,25</sup> which corresponds well with the operating range of commercially available gels like Bio-Beads S-X1. Figure 3 shows a photograph of the SEC column during separation. Just after loading, the polydisperse sample gave rise to a black band about 2 cm-long. During the separation, this black band became increasingly broad showing that the average size of the nanoparticles is smaller than the exclusion limit of the beads that were used. Finally, five fractions with

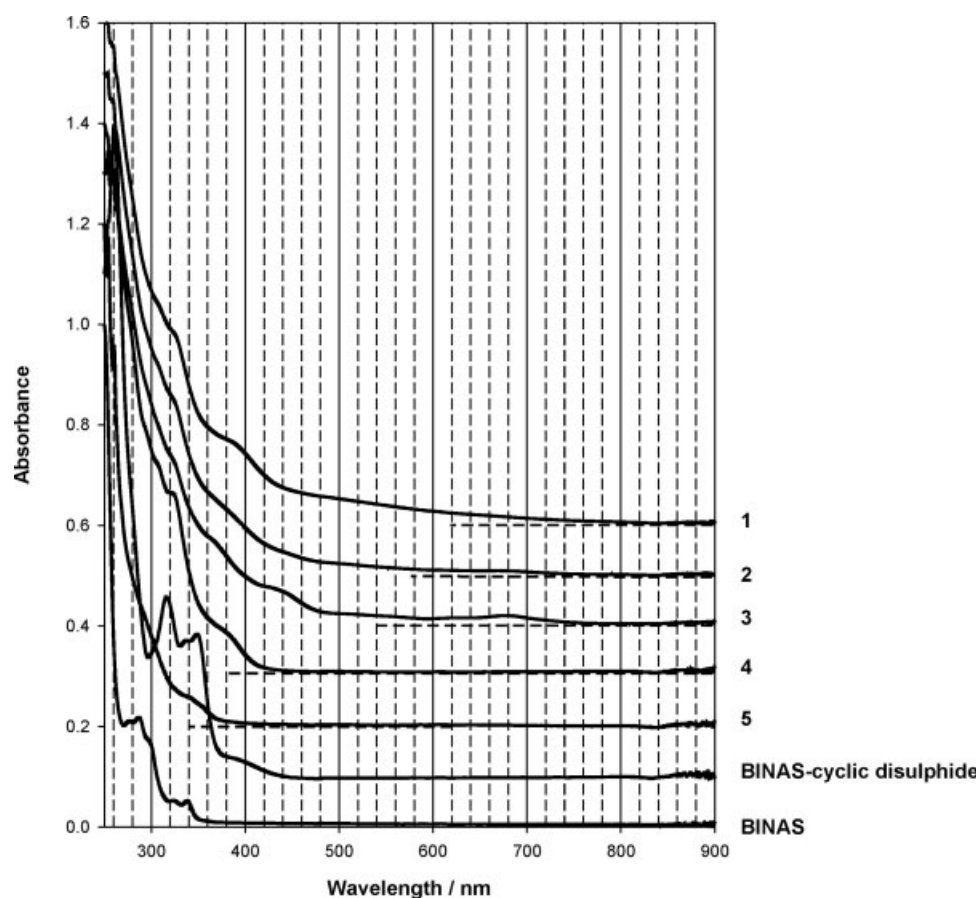


**Fig. 2.** UV-vis spectra of the separated fractions 1–5. Spectra are offset for clarity and normalized to one absorbance unit at 250 nm. The bottom spectrum corresponds to BINAS and the second one to BINAS-cyclic disulphide.



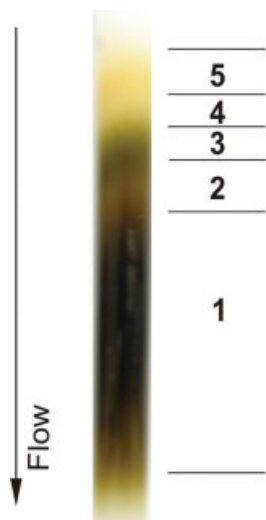


**Fig. 3.** Size exclusion chromatography separation of BINAS protected gold particles. The separated fractions are numbered from 1–5 according to their decreasing elution mobility. Horizontal lines show roughly the limit between adjacent fractions. [Color figure can be viewed in the online issue, which is available at [www.interscience.wiley.com](http://www.interscience.wiley.com).]

different color could be separated and were numbered 1–5 according to their elution order or their decreasing size. This shows that the size distribution is not homogenous and indicates the presence of magic number compounds, i.e., the high relative abundance of compounds with well-defined composition. The dependence of color on the size is a direct consequence of a quantum size effect. The latter is also responsible for the systematic red shift of the absorption onset for increasing particle size (from 5 to 1). Fractions 1, 3, and 5 are respectively brown, green, and yellow. Fraction 2 seems to be a mixture of the adjacent fractions 1 and 3 as judged from the UV-vis and CD spectra (vide infra).

#### Nuclear Magnetic Resonance of Gold BINAS Nanoparticles

The upper part of Figure 4 shows the aromatic region of  $^1\text{H}$  NMR spectra for polydisperse gold nanoparticles covered with BINAS, free BINAS, and dithiophene[2,1-c:1',2'-e] $^{1,2}$ dithiin (BINAS-cyclic disulphide) (Chart 1). The lower part of the Figure compares the aliphatic part of both TOAB and the as-prepared gold nanoparticles. In the aromatic region, the  $^1\text{H}$  NMR spectrum of unbound BINAS displays six sets of signals with chemical shifts  $\delta$  (ppm) = 7.89 (d, 2 H), 7.88 (d, 2 H), 7.55 (d, 2 H), 7.41 (m, 2 H), 7.28 (m, 2 H), 6.98 (d, 2 H) and BINAS-cyclic disulphide shows five sharp signals,  $\delta$  (ppm) = 7.90 (d, 2 H), 7.84 (2d, 2 H), 7.79 (d, 2 H), 7.44 (ddd, 2 H), 7.22–7.14 (m, 4 H). BINAS-cyclic disulphide is a major by-product observed during the synthesis of BINAS-gold nanoparticles. In contrast to the sharp signals observed for the latter compounds, the polydisperse gold nanoparticles are characterized by broad and shifted signals. This observation leads us to conclude that after purification the sample is free from BINAS-cyclic disulphide and BINAS impur-

ities. Previous  $^1\text{H}$  NMR studies<sup>26–30</sup> of MPNs have also described significant peak broadening and four main explanations have been put forward: (a) Rapid spin–spin relaxation from dipolar interaction; (b) dependence of chemical shifts on the size of nanoparticles and on the type of binding site (vertex, edges, terraces); (c) size-dependent rotation diffusion of the cluster leading to size-dependent spin–spin relaxation broadening; (d) the oxidation states of nanoparticles have a significant effect on NMR spectra of the monolayer ligand shell. The aliphatic part of the  $^1\text{H}$  NMR spectra reveals the presence of tetraoctylammonium groups, which have a NMR signature significantly different from the one of free TOAB. This shows that there is no free TOAB. It has been shown by mass spectroscopy that the tetraoctylammonium groups balance the negative charge on the Au-thiolate cores.<sup>31</sup>

#### UV-vis Spectra

The UV-vis spectra in Figure 2 of the separated samples show no sign of a surface plasmon resonance characteristic for particles equal or larger to 3 nm, in agreement with the TEM measurements. However, the absorption spectra of the different fractions 1–5 show considerable structure. Also, the absorption spectra are distinctly different from the ones observed for the free BINAS and BINAS-cyclic disulphide ligands. There is also a clear trend in the spectra as concerns the absorption onset, which shifts to longer wavelengths with increasing particle size. This trend has already been observed for gold particles covered by glutathione<sup>14,25</sup> and *N*-isobutyl-L-cysteine,<sup>11</sup> respectively, separated into different compounds by gel electrophoresis. For example, the onset of absorption occurred at about 400 nm for particles containing 10–12 gold core

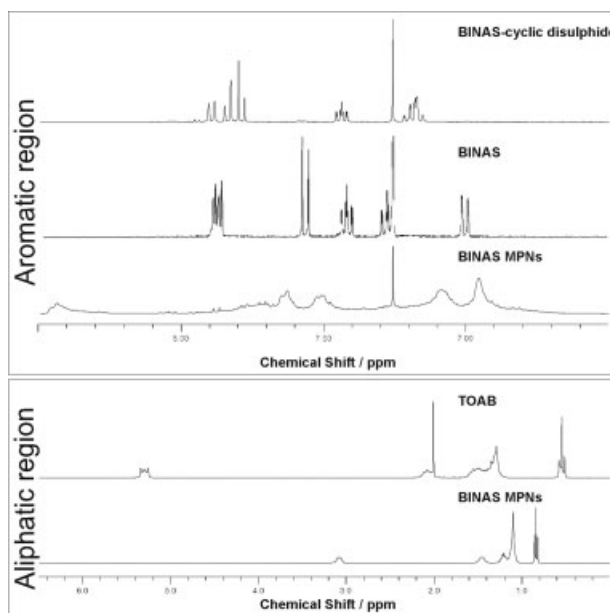


**Fig. 4.**  $^1\text{H}$  NMR spectra (top) in the aromatic region of the polydisperse nanoparticles covered with BINAS, free BINAS and BINAS-cyclic disulphide and  $^1\text{H}$  NMR spectra (bottom) in the aliphatic part of the polydisperse nanoparticles and of TOAB.

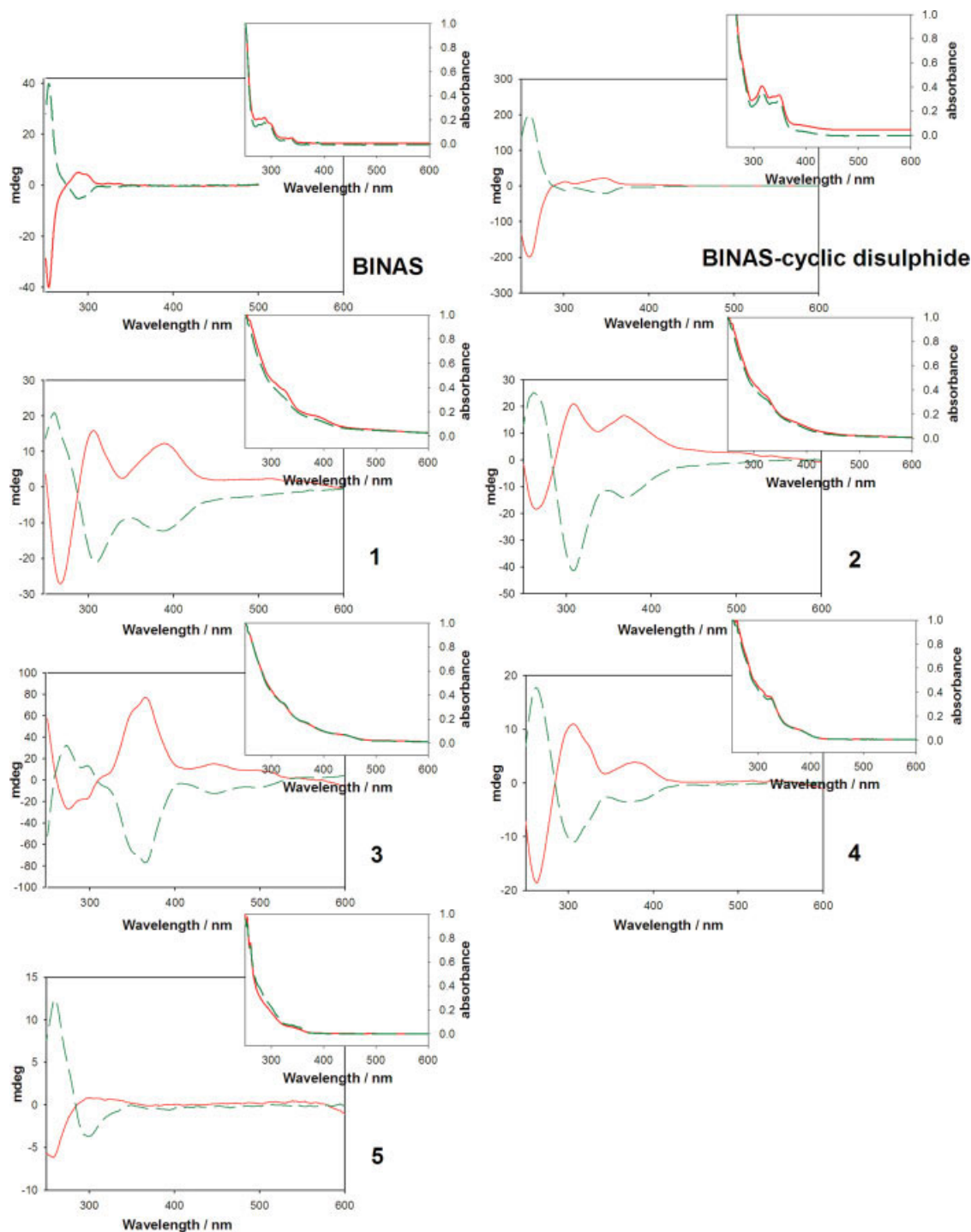
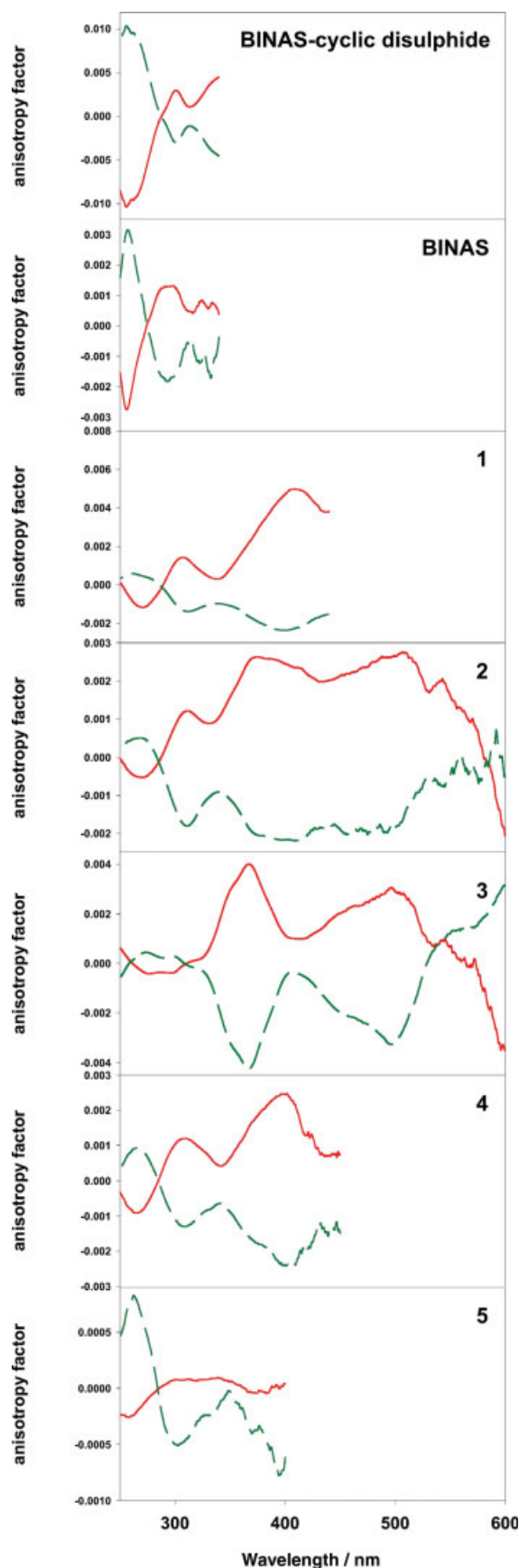


**Fig. 5.** CD and UV-vis spectra of separated fractions **1–5** of gold particles covered with *S*-BINAS (dashed) and *R*-BINAS (solid line). The UV-vis spectra were scaled to 1 absorbance unit at 250 nm. [Color figure can be viewed in the online issue, which is available at [www.interscience.wiley.com](http://www.interscience.wiley.com).]

atoms and above 800 nm for 25 gold core atoms. This indicates that the particles investigated here are very small, containing ten to a few tens of gold atoms only. Interestingly, the onset of absorption of particles containing 10 or 12 gold atoms depends strongly on the nature of the ligand. For  $\text{Au}_{11}$  covered by phosphine ligands, the *Chirality* DOI 10.1002/chir

absorption onset is found at around 600 nm,<sup>17</sup> whereas for gold particles of similar size covered by thiols it is found at around 400 nm.<sup>25</sup> This may be a consequence of the different nature of the gold–phosphorus and gold–sulfur bonds, the latter being considerably stronger. This likely has also an influence on the structure of the metal core. The struc-



ture of Au<sub>11</sub> covered by phosphine ligands is well-known from X-ray crystallography,<sup>32,33</sup> which reveals a compact metal core with a central gold atom surrounded by 10 peripheral gold atoms. The structure of gold particles of similar size covered by thiols might however be quite different. Indeed, density functional theory (DFT) calculations indicate that the structure of such small gold cores is strongly distorted by the adsorbing thiol. In particular, based on DFT calculations, the formation of cyclic thiolated gold clusters has been proposed.<sup>34</sup>

#### Optical Activity in the UV-vis

Figure 5 shows the CD spectra of the separated fractions. The CD spectra of the gold particles covered with BINAS are distinctly different from the CD spectra of both free BINAS and BINAS-cyclic disulphide. It is, therefore, concluded that the optical activity observed for the gold particles covered by the BINAS is associated with electronic transitions within the metal core. It is also evident that the CD spectra depend on the particle size. This is particularly apparent from a comparison between the CD spectra of fractions **1** and **3**. None of the CD spectra is similar to those reported for small gold particles covered by the water-soluble thiols glutathione,<sup>14</sup> penicillamine<sup>15</sup> and *N*-isobutyl-cysteine,<sup>11</sup> respectively.

Optical activity of gold particles covered by BINAS has not yet been reported. However, two independent studies report the CD spectra of gold nanoparticles protected by BINAP.<sup>16,17</sup> The protocol for the preparation of these particles was quite different in the two cases. In the procedure proposed by Hutchison and coworkers,<sup>35</sup> HAuCl<sub>4</sub> was reduced in the presence of the BINAP. This resulted in small particles with a size of  $1.7 \pm 0.4$  nm, according to TEM. The other procedure started from a Au<sub>2</sub>Cl<sub>2</sub> (BINAP) precursor that was subsequently reduced. This resulted selectively in Au<sub>11</sub> clusters, as supported by electrospray ionization mass spectrometry and in agreement with TEM.<sup>17</sup> The CD spectra reported for these two compounds are strikingly similar despite the fact that the average size of the particles in the former study is considerably larger. For the particles covered with the *R*-enantiomer of the BINAP, the CD spectra reported in both studies are characterized by a positive band at 440 nm, an about twice as strong positive band at 350 nm with a shoulder at longer wavelength and an even stronger negative band slightly below 300 nm. The striking similarity of these spectra indicates that the optical activity originates from similar particles within the two samples. Since the average size of the two samples is rather different and since in one case the sample consisted predominantly of Au<sub>11</sub> clusters, it is proposed that the sample with the larger average size particles contains Au<sub>11</sub> clus-

**Fig. 6.** Anisotropy factor of fractions **1**–**5** of BINAS gold nanoparticles, BINAS, and BINAS-cyclic disulphide. Dashed (solid) spectra are for the *S*-enantiomer (*R*-enantiomer). The anisotropy factor of fractions **1** and **5** is not symmetric for the two enantiomers because these fractions contain mixtures of different particles. [Color figure can be viewed in the online issue, which is available at [www.interscience.wiley.com](http://www.interscience.wiley.com).]



ters, which leads to the observed optical activity. This furthermore implies that the larger particles, around 1.7 nm in size, do not contribute much to the optical activity of the sample.

Comparison of the CD spectra of the gold BINAP particles described above with the ones reported here for the gold BINAS particles shows for example that fraction **3** has a completely different CD spectrum. On the other hand fraction **4** exhibits a CD spectrum with similar shape and sign as that for Au<sub>11</sub> covered by BINAP, but shifted to shorter wavelength by about 50 nm. For the *R* enantiomer, a positive band at 380 nm, an about two and a half times as strong positive band at 300 nm with a shoulder at longer wavelengths and an even stronger negative band at 260 nm are observed. The corresponding UV-vis spectra also bear the same similarity with discrete bands shifted to longer wavelengths for the gold particles covered by the BINAS. For the gold particles covered by the BINAP (BINAS, fraction **4**) bands in the absorption spectra are observed at about 440 nm (380 nm), 370 nm (325 nm), and 350 nm (305 nm). These similarities could of course arise by chance, but they can also be an indication that fraction **4** contains Au<sub>11</sub> clusters covered by BINAS and that these Au<sub>11</sub> clusters have a similar structure as the ones covered by BINAP. The shift of the CD and absorption spectra has likely to do with the different nature of the gold-sulfur and gold-phosphorus bond. For such small clusters as Au<sub>11</sub> almost all the gold atoms reside on the surface of the metal particle and therefore the adsorbate has a strong influence on its electronic structure. For example, the latter is influenced by charge transfer between gold particles and adsorbate, which depends on the nature of the adsorbate.

It has been proposed that the optical activity of the Au<sub>11</sub> clusters covered by BINAP is due to an intrinsically chiral core.<sup>17</sup> It is known that the structure of the Au<sub>11</sub> core depends on the type of the phosphine ligands.<sup>36</sup> This has probably to do with the fact that 10 of the 11 gold atoms reside on the surface of the metal core. The atoms are therefore unsaturated and relatively flexible. Adsorption of the BINAP leads to a deformation of the core to an asymmetric structure, which is at the origin of the optical activity in metal-based transitions. Such deformations are likely favored by molecules that contain two or more functional groups that can interact with the gold core. Our findings are in agreement with such a model. Since the gold-sulfur bond is stronger than the gold-phosphorus bond, the distortion of the gold core imposed by the adsorbed ligand is expected to be stronger in the case of adsorbed BINAS compared with adsorbed BINAP. This could also lead to a stronger deviation from a symmetric structure in the former case and therefore to a stronger chiroptical response. Indeed, the anisotropy factors ( $\Delta\epsilon/\epsilon$ ) found here for fraction **4** of gold particles covered by BINAS are about a factor of two stronger than the ones reported for Au<sub>11</sub> covered by BINAP.<sup>17</sup> In both cases, the band at the longest wavelength has the largest anisotropy factor (see Fig. 6), which is  $1.2 \times 10^{-3}$  in the latter and  $2.5 \times 10^{-3}$  in the former case. Note that anisotropy factors as large as  $4.0 \times 10^{-3}$  are found for fraction **3**. To the best of our knowl-

edge such large anisotropy factors were never observed for optically active gold particles.

In conclusion, we report the preparation of small gold particles passivated by BINAS. The as prepared and purified particles could be separated into several distinct fractions using size-exclusion chromatography. The different fractions exhibit different color, absorption and CD spectra. The absorption and CD spectra of one fraction bears some resemblance with the spectra previously reported for Au<sub>11</sub> particles stabilized by BINAP although the spectra are shifted to shorter wavelength in the case of the thiol. The anisotropy factors are as large as  $4 \times 10^{-3}$ , which is the largest reported so far for gold particles covered by chiral thiols. This indicates that BINAS is particularly well-suited to bestow chirality onto gold particles. The results show that the optical activity is enhanced by using a stronger gold-ligand bond. This is in good agreement with a model that ascribes the optical activity to an adsorbate-induced local deformation of the metal core, i.e., the formation of a "chiral-footprint."<sup>11</sup>

## ACKNOWLEDGMENTS

The authors thank Julien Boudon and Natallia Shalkevich for TEM measurements.

## LITERATURE CITED

1. Daniel MC, Astruc D. Gold nanoparticles: assembly, supramolecular chemistry, quantum-size-related properties, and applications toward biology, catalysis, and nanotechnology. *Chem Rev* 2004;104:293-346.
2. Bond GC. Gold: a relatively new catalyst. *Catal Today* 2002;72:5-9.
3. Storhoff JJ, Elghanian R, Mucic RC, Mirkin CA, Letsinger RL. One-pot colorimetric differentiation of polynucleotides with single base imperfections using gold nanoparticle probes. *J Am Chem Soc* 1998;120:1959-1964.
4. West JL, Halas NJ. Engineered nanomaterials for biophotonics applications: improving sensing, imaging, and therapeutics. *Ann Rev Biomed Eng* 2003;5:285-292.
5. Zharov VP, Letfullin RR, Galitovskaya EN. Microbubbles-overlapping mode for laser killing of cancer cells with absorbing nanoparticle clusters. *J Phys D: Appl Phys* 2005;38:2571-2581.
6. Sun S, Murray CB, Weller D, Folks L, Moser A. Monodisperse FePt nanoparticles and ferromagnetic FePt nanocrystal superlattices. *Science* 2000;287:1989-1992.
7. Barnes WL, Dereux A, Ebbesen TW. Surface plasmon subwavelength optics. *Nature* 2003;424:824-830.
8. Schaaff TG, Shafigullin MN, Khoury JT, Vezmar I, Whetten RL, Cullen WG, First PN, GutierrezWing C, Ascensio J, JoseYacaman MJ. Isolation of smaller nanocrystal Au molecules: robust quantum effects in optical spectra. *J Phys Chem B* 1997;101:7885-7891.
9. Chen SW, Ingram RS, Hostetler MJ, Pietron JJ, Murray RW, Schaaff TG, Khoury JT, Alvarez MM, Whetten RL. Gold nanoelectrodes of varied size: transition to molecule-like charging. *Science* 1998;280:2098-2101.
10. Gautier C, Burgi T. Vibrational circular dichroism of *N*-acetyl-L-cysteine protected gold nanoparticles. *Chem Commun* 2005:5393-5395.
11. Gautier C, Burgi T. Chiral *N*-isobutyl-L-cysteine protected gold nanoparticles: preparation, size selection, and optical activity in the UV-vis and infrared. *J Am Chem Soc* 2006;128:11079-11087.
12. Bieri M, Burgi T. Adsorption kinetics, orientation, and self-assembling of *N*-acetyl-L-cysteine on gold: a combined ATR-IR, PM-IRRAS, and QCM study. *J Phys Chem B* 2005;109:22476-22485.
13. Schaaff TG, Knight G, Shafigullin MN, Borkman RF, Whetten RL. Isolation and selected properties of a 10.4 kDa gold: glutathione cluster compound. *J Phys Chem B* 1998;102:10643-10646.

14. Schaaff TG, Whetten RL. Giant gold-glutathione cluster compounds: intense optical activity in metal-based transitions. *J Phys Chem B* 2000;104:2630–2641.
15. Yao H, Miki K, Nishida N, Sasaki A, Kimura K. Large optical activity of gold nanocluster enantiomers induced by a pair of optically active penicillamines. *J Am Chem Soc* 2005;127:15536–15543.
16. Tamura M, Fujihara H. Chiral bisphosphine BINAP-stabilized gold and palladium nanoparticles with small size and their palladium nanoparticle-catalyzed asymmetric reaction. *J Am Chem Soc* 2003;125:15742–15743.
17. Yanagimoto Y, Negishi Y, Fujihara H, Tsukuda T. Chiroptical activity of BINAP-stabilized undecagold clusters. *J Phys Chem B* 2006;110:11611–11614.
18. Li TH, Park HG, Lee HS, Choi SH. Circular dichroism study of chiral biomolecules conjugated nanoparticles. *Nanotechnology* 2004;15: S660–S663.
19. Shemer G, Krichevski O, Markovich G, Molotsky T, Lubitz I, Kotlyar AB. Chirality of silver nanoparticles synthesized on DNA. *J Am Chem Soc* 2006;128:11006–11007.
20. Garzon IL, Reyes-Nava JA, Rodriguez-Hernandez JI, Sigal I, Beltran MR, Michaelian K. Chirality in bare and passivated gold nanoclusters. *Phys Rev B* 2002;66:073403.
21. Goldsmith MR, George CB, Zuber G, Naaman R, Waldeck DH, Wipf P, Beratan DN. The chiroptical signature of achiral metal clusters induced by dissymmetric adsorbates. *Phys Chem Chem Phys* 2006;8:63–67.
22. Hashmi ASK, Hutchings GJ. Gold catalysis. *Angew Chem Int Ed* 2006;45:7896–7936.
23. Fabbri D, Delogu G, De Lucchi O. Preparation of enantiomerically pure 1,1'-binaphthalene-2,2'-diol and 1,1'-binaphthalene-2,2'-dithiol. *J Org Chem* 1993;58:1748–1750.
24. Brust M, Walker M, Bethell D, Schiffrin DJ, Whyman R. Synthesis of thiol-derivatized gold nanoparticles in a 2-phase liquid–liquid system. *J Chem Soc Chem Commun* 1994:801–802.
25. Negishi Y, Nobusada K, Tsukuda T. Glutathione-protected gold clusters revisited: bridging the gap between gold(I)-thiolate complexes and thiolate-protected gold nanocrystals. *J Am Chem Soc* 2005;127:5261–5270.
26. Donkers RL, Lee D, Murray RW. Synthesis and isolation of the molecule-like cluster  $\text{Au}_{38}(\text{PhCH}_2\text{CH}_2\text{S})_{24}$ . *Langmuir* 2004;20:1945–1952.
27. Hostetler MJ, Wingate JE, Zhong CJ, Harris JE, Vachet RW, Clark MR, Londono JD, Green SJ, Stokes JJ, Wignall GD, Glish GL, Porter MD, Evans ND, Murray RW. Alkanethiolate gold cluster molecules with core diameters from 1.5 to 5.2 nm: core and monolayer properties as a function of core size. *Langmuir* 1998;14:17–30.
28. Badia A, Gao W, Singh S, Demers L, Cuccia L, Reven L. Structure and chain dynamics of alkanethiol-capped gold colloids. *Langmuir* 1996;12:1262–1269.
29. Badia A, Lennox RB, Reven L. A dynamic view of self-assembled monolayers. *Acc Chem Res* 2000;33:475–481.
30. Song Y, Harper AS, Murray RW. Ligand heterogeneity on monolayer protected gold clusters. *Langmuir* 2005;21:5492–5500.
31. Price RC, Whetten RL. All-aromatic, nanometer-scale, gold-cluster Thiolate Complexes. *J Am Chem Soc* 2005;127:13750–13751.
32. Albano VG, Bellon PL, Manassero M, Sansoni M. Intermetallic pattern in metal-atom clusters—structural studies on  $\text{Au}_{11}\text{X}_3(\text{Pr}_3)_7$  species. *J Chem Soc Chem Commun* 1970:1210–1211.
33. Bos W, Kanters RPF, Vanhalen CJ, Bosman WP, Behm H, Smits JMM, Beurskens PT, Bour JJ, Pignolet LH. Gold clusters—synthesis and characterization of  $[\text{Au}-8(\text{PPh}_3)_7(\text{CNR})]^{2+}$ ,  $[\text{Au}-9(\text{PPh}_3)_6(\text{CNR})_2]^{3+}$  and  $[\text{Au}-11(\text{PPh}_3)_7(\text{CNR})_2\text{I}]^{2+}$  and their reactivity towards amines—the crystal-structure of  $[\text{Au}-11(\text{PPh}_3)_7(\text{CN}-\text{I}-\text{Pr})_2\text{I}](\text{PF}_6)_2$ . *J Organomet Chem* 1986;307:385–398.
34. Hakkinen H, Walter M, Gronbeck H. Divide and protect: capping gold nanoclusters with molecular gold-thiolate rings. *J Phys Chem B* 2006;110:9927–9931.
35. Weare WW, Reed SM, Warner MG, Hutchison JE. Improved synthesis of small (d(CORE) approximate to 1.5 nm) phosphine-stabilized gold nanoparticles. *J Am Chem Soc* 2000;122:12890–12891.
36. Nunokawa K, Onaka S, Yamaguchi T, Ito T, Watase S, Nakamoto M. Synthesis and characterization of the  $\text{Au}_{11}$  cluster with sterically demanding phosphine ligands by single crystal X-ray diffraction and XPS spectroscopy. *Bull Chem Soc Jpn* 2003;76:1601–1602.